

Theory of the dynamic magnetic response of $\text{Ce}_3\text{Bi}_4\text{Pt}_3$: A heavy-fermion semiconductor

Peter S. Riseborough

Department of Physics, Polytechnic University, 333 Jay Street, Brooklyn, New York 11201

(Received 26 December 1991)

The properties of the semiconducting phase of heavy-fermion systems are examined within the framework of mean-field theory. The theory exhibits the possibility of a transition from a high-temperature local-moment state to a low-temperature, semiconducting state. The low-temperature, semiconducting state has an indirect band gap that is reduced by many-body renormalizations. The magnetic properties of this system are examined within this mean-field approximation and are compared with the results of recent inelastic-neutron-scattering experiments.

I. INTRODUCTION

Heavy-fermion systems form a class of materials that are all characterized by extremely strong electronic correlations,¹⁻⁴ as evidenced by large enhancements of the low-temperature specific heats and static magnetic susceptibilities above the values expected from local-density approximation (LDA) electronic-structure calculations. Even though the properties of heavy-fermion systems are generically similar at moderately low temperatures, the class of systems encompasses a wide variety of different ground states, including superconductivity, spin density waves, charge density waves, and simple itinerant paramagnetism. Recently, another class of such systems has emerged,⁵⁻¹² namely that of heavy-fermion semiconductors. Their properties may be characterized as usual heavy-fermion systems at moderately low temperatures, but at very low temperatures they enter into a ground state in which the electronic excitations have a minimum or threshold excitation energy.

In this paper we shall investigate the properties of the standard model of heavy-fermion systems,¹³⁻¹⁶ in the mean-field slave-boson approximation,¹⁷⁻²⁶ and outline schematically how such a semiconducting ground state may evolve. Although fluctuation effects are expected to yield important corrections to the mean-field approximation, we expect that the qualitative nature of the mean-field state will be maintained.

We shall explicitly evaluate the dynamical susceptibility in this model, and then compare the results of the theory with data from inelastic-neutron-scattering experiments⁶ on $\text{Ce}_3\text{Bi}_4\text{Pt}_3$, which is an example of a low-temperature semiconductor,^{6,7} which is subject to moderate many-body enhancements.

The paper is structured as follows: In Sec. II, we shall describe the theoretical model for the cerium-based heavy-fermion systems and introduce the electronic correlations via the technique involving slave bosons. In Sec. III, we shall present the mean-field approximation to the solution of the model. This involves a phase transition in which the slave bosons form a condensate.¹⁹⁻²² In the low-temperature phase found in the mean-field approximation, the f excitations weakly hybridize with the

conduction band and form a semiconductor with renormalized bands. Whereas at high temperatures, the f excitations are completely decoupled from the conduction band. Both the complete decoupling found at high temperatures and the sharp phase transition are unphysical artifacts, but are expected to be corrected by treatments that incorporate the effect of fluctuations. We shall present the electronic structure calculated within the mean-field approximation. In Sec. IV we examine the magnetic properties and compare them with experiments. We discuss and summarize our results in Sec. V.

II. THE PERIODIC ANDERSON MODEL

The properties of cerium heavy-fermion systems are unusual due to the following facts: The $4f$ orbitals in the lanthanide series have a small spatial extent, but the $4f$ shell is only partially filled. Due to the small radius of the $4f$ orbitals, the electrons in the $4f$ level experience strong Coulomb interactions with the other electrons in the $4f$ shell. In cerium ions the $4f^0$ and the $4f^1$ configurations have almost the same energy, due to the stability of closed atomic shells. In the solid, these neighboring configurations can be mixed by the potential due to the other atoms, thereby allowing a $4f$ electron to escape into the conduction band. These peculiarities are incorporated in the simplest model of cerium heavy-fermion systems, the Anderson lattice Hamiltonian.

The total Hamiltonian is written as the sum of three parts,

$$H = H_f + H_d + H_{f-d} . \quad (1)$$

The f electrons are governed by H_f , where

$$H_f = \sum_{i,m} E_f f_{i,m}^\dagger f_{i,m} + \frac{1}{2} \sum_{i,m,n} U_{ff} f_{i,m}^\dagger f_{i,n}^\dagger f_{i,n} f_{i,m} \quad (1a)$$

and $f_{i,m}^\dagger$ and $f_{i,m}$, respectively, create and annihilate an f electron in the $4f$ shell at lattice site i , in the orbital labeled by the set of quantum numbers n . The degeneracy of the $4f$ level is $N = 2l(l+1) = 14$. The term proportional to E_f represents the binding energy of the $4f$ electrons, while the term proportional to U_{ff} is the Coulomb repulsion between pairs of electrons in the $4f$ shell of the same

ion. The Pauli exclusion principle leads to the exclusion of the term where $m = n$.

The conduction band is governed by the Hamiltonian H_d ,

$$H_d = \sum_{\mathbf{k}, m} e(\mathbf{k}) d_{\mathbf{k}, m}^\dagger d_{\mathbf{k}, m}, \quad (1b)$$

where $d_{\mathbf{k}, m}^\dagger$ and $d_{\mathbf{k}, m}$, respectively, create and annihilate electrons in the conduction-band state labeled by Bloch wave vector \mathbf{k} and degeneracy index m .

The f - d mixing term is

$$H_{f-d} = N_s^{-1/2} \sum_{i, \mathbf{k}, m} [V \exp(i\mathbf{k} \cdot \mathbf{R}_i) f_{i, m}^\dagger d_{\mathbf{k}, m} + V^* \exp(-i\mathbf{k} \cdot \mathbf{R}_i) d_{\mathbf{k}, m}^\dagger f_{i, m}]. \quad (1c)$$

The first term takes an electron out of the d band and places it in the $4f$ orbital at site i , and the second term represents the opposite process. In the above expression the number of lattice sites in the crystal is denoted by N_s . Thus, apart from the term proportional to U_{ff} the Hamiltonian is quadratic in the fermion operators, and the terms of (1b), and (1c) provide dispersion to the $4f$ levels. The term proportional to U_{ff} is local and quartic in the fermion operators.

In general dimensions, this model is intractable and only possesses two exactly soluble limits, the weak coupling limit and the atomic limit. We shall, therefore, examine this model within a mean-field approximation, which has its validity based on the limit of large degeneracy N . We shall then specifically examine the situation in which the system is in a semiconducting phase at low temperatures.

The Coulomb interaction U_{f-f} is the largest term in the Hamiltonian, and often it is considered to be infinite. In this case normal perturbation theory is not appropriate and other techniques have to be utilized.¹³⁻¹⁸ Since cerium compounds usually have an average of less than one $4f$ electron in the f shell of each ion, in the large- U_{ff} limit it is reasonable to project out states in which the $4f$ shell is occupied by more than one electron, leaving only the $4f^0$ and $4f^1$ configurations. This projection must be performed for all states involved in the calculation, including intermediate states. This minimizes the Coulomb interaction part of the Hamiltonian; in fact this procedure leads to the term proportional to U_{ff} vanishing. When this minimization is performed the terms quartic in the fermion operators, in the above Hamiltonian, will be eliminated but only at the expense of introducing a new boson field. We shall now outline the method of projection that we shall follow.

Slave-boson Hamiltonian

The projection of the multiply occupied configurations is accomplished by the introduction of slave bosons introduced by Barnes¹⁷ and independently rediscovered by Coleman.¹⁸ A slave-boson creation and annihilation operator b_i^\dagger and b_i is introduced for each lattice site. At each site the constraint

$$Q_i = b_i^\dagger b_i + \sum_m f_{i, m}^\dagger f_{i, m} = 1 \quad (2)$$

is to be enforced. Due to the positive definite nature of the slave-boson number operators, this restriction enforces the number of f electrons on each site to be less than unity.

The number of bosons represents the number of $4f^0$ configurations. The second term is the number of $4f^1$ configurations. The constraint (2) enforces the condition that each $4f$ ion is in either one configuration or the other. The $4f$ configurations are represented by

$$|4f_i^0\rangle = b_i^\dagger |0\rangle$$

and

$$|4f_i^1\rangle = f_{i, m}^\dagger |0\rangle.$$

Thus, in this restricted part of Hilbert space the physical f operators are formed by the product of a quasiparticle f operator and a slave-boson operator, the latter factor represents the charge fluctuations of the f shell. The hybridization or mixing term is then replaced by

$$H'_{f-d} = N_s^{-1/2} \sum_{i, \mathbf{k}, m} [V \exp(i\mathbf{k} \cdot \mathbf{R}_i) f_{i, m}^\dagger d_{\mathbf{k}, m} b_i + V^* \exp(-i\mathbf{k} \cdot \mathbf{R}_i) b_i^\dagger d_{\mathbf{k}, m}^\dagger f_{i, m}] \quad (3)$$

since it has to take an electron out of the band and change the $4f$ ionic configuration from $|4f_i^0\rangle$ to $|4f_i^1\rangle$ and vice versa.

The partition function Z is given by

$$Z = \text{Tr} \exp(-H/k_B T), \quad (4)$$

which is projected onto the manifold of singly occupied $4f$ sites via

$$Z = \text{Tr} \Pi_i \delta(Q_i - 1) \exp(-H'/k_B T), \quad (5)$$

where the Hamiltonian H' represents the Hamiltonian H in which the hybridization term (1c) has been replaced by the expression given in Eq. (3). Using the integral representation of the δ function yields

$$Z = \text{Tr} \Pi_i \int d\eta_i \exp \left[i \sum_i \eta_i (Q_i - 1) - H'/k_B T \right] \quad (6)$$

and on setting η_i to the saddle-point values $\eta_i = i\lambda_i/k_B T$, we obtain an effective Hamiltonian with the constraint automatically built in.

The projected Hamiltonian H_p , which includes the constraint, finally becomes,¹⁷⁻²⁵

$$H_p = \sum_{i, m} E_f f_{i, m}^\dagger f_{i, m} + \sum_{\mathbf{k}, m} e(\mathbf{k}) d_{\mathbf{k}, m}^\dagger d_{\mathbf{k}, m} + H'_{f-d} + \sum_i \lambda_i (1 - Q_i). \quad (7)$$

This Hamiltonian has the same matrix elements as the initial one, as long as one stays within the manifold of states, which satisfies the constraints. This Hamiltonian is quadratic in the fermion operators as the Coulomb interaction term has been projected out, however the hybridization term in (3) is of cubic order in the number of

operators. The effect of the slave bosons is to prohibit an electron hopping onto an f orbital if it is already in a $4f^1$ configuration. This is accomplished by the presence of the local boson destruction operator, which when it acts on the $4f^1$ configuration, yields zero, since this state corresponds to the vacuum state for the local boson.

The slave bosons satisfy the equation of motion

$$\begin{aligned} i\hbar\partial_t b_i^\dagger(t) &= [b_i^\dagger(t), H_p(t)]_- \\ &= \lambda_i b_i^\dagger(t) - VN_s^{-1/2} \sum_{\mathbf{k}, m} \exp(i\mathbf{k}\cdot\mathbf{R}_i) \\ &\quad \times f_{i,m}^\dagger(t) d_{\mathbf{k},m}(t). \end{aligned} \quad (8)$$

Note that the Hamiltonian commutes with the constraints and with the number operator then, as found from the Heisenberg equations of motion

$$i\hbar\partial_t Q_i = [Q_i, H_p]_- = 0. \quad (9)$$

The constraint is conserved and so it only has to be imposed at just one instant of time. Thus, the slave bosons impose a dynamical constraint on the f electron charge fluctuations.

The boson operators are replaced by the sum of complex number a_0 and an operator B_i representing the remaining fluctuations,

$$b_i^\dagger = a_0^* + B_i^\dagger$$

and

$$b_i = a_0 + B_i.$$

The phase of the complex number could have been chosen to be different at different sites, however, this could be gauged away in all physical quantities by also performing a local gauge transformation on the f quasiparticle operators. That is, the complex boson field and f are operators that could be replaced according to the rules

$$a_0 \Rightarrow a_0' \exp(+i\psi_i)$$

and

$$f_i \Rightarrow f_i' \exp(+i\psi_i). \quad (10)$$

Thus, the local gauge field neither enters into the Hamiltonian nor any other physical quantity, but the fluctuations of the global phase do represent a soft mode that could smooth out any mean-field phase transition for finite values of N . However even in this case, it may be argued that the qualitative behavior found within the mean-field approximation does remain unaltered.^{20,21}

III. THE MEAN-FIELD APPROXIMATION

The mean-field slave-boson approximation corresponds to neglecting the fluctuating parts B_i of the boson operators. Thus, we consider the state found by utilizing the approximation,

$$b_i^\dagger = b_i = a_0.$$

This corresponds to a macroscopic occupation of the uni-

form $\mathbf{k}=0$ state of the slave bosons if a_0 is finite. Thus, the state with a nonzero a_0 is a bose-condensed phase where fluctuations in the number of bosons may be neglected. It also corresponds to the semiclassical approximation for the boson field, which is often used in electrodynamics. Thus, the boson field is replaced by a classical field. Since a_0 is assumed to be time independent, then the expectation value of the equation of motion becomes

$$i\hbar\partial_t a_0 = 0, \quad (11a)$$

which yields the equation

$$a_0 \lambda_i = VN_s^{-1/2} \sum_{\mathbf{k}, m} \exp(i\mathbf{k}\cdot\mathbf{R}_i) \langle f_{\mathbf{k},m}^\dagger d_{\mathbf{k},m} \rangle. \quad (11b)$$

In this mean-field approximation the Hamiltonian has become quadratic in the fermion operators, and the boson operators have been approximated by scalars, although their values are still to be determined. Therefore, the fermion part of the Hamiltonian can be diagonalized, yielding the electronic structure. This is performed by calculating the single fermion Green's functions.

Electronic structure. The one-electron Green's functions are defined by

$$G_{i,m;i',m'}^{ff}(t) = -(i/\hbar) \langle \mathcal{T} f_{i,m}(t) f_{i',m'}^\dagger(0) \rangle \quad (12a)$$

for the f electrons and similarly for the d electrons

$$G_{\mathbf{k},m;\mathbf{k}',m'}^{dd}(t) = -(i/\hbar) \langle \mathcal{T} d_{\mathbf{k},m}(t) d_{\mathbf{k}',m'}^\dagger(0) \rangle. \quad (12b)$$

The f - d Green's function is given by

$$G_{\mathbf{k},m;\mathbf{k}',m'}^{df}(t) = -(i/\hbar) \langle \mathcal{T} d_{\mathbf{k},m}(t) f_{\mathbf{k}',m'}^\dagger(0) \rangle, \quad (12c)$$

where \mathcal{T} is Wick's time-ordering operator, and the angular brackets indicate the average.

The one-electron Green's functions are found from the equations of motion, which result in the pair of coupled differential equations

$$\begin{aligned} (i\hbar\partial_t - \bar{E}_f) G_{i,m;i',m'}^{ff}(t) &= \delta(t) \delta_{i,m;i',m'} \\ &\quad + VN_s^{-1/2} \sum_{\mathbf{k}} a_0 \exp(i\mathbf{k}\cdot\mathbf{R}_i) \\ &\quad \times G_{\mathbf{k},m;i',m'}^{df}(t) \end{aligned} \quad (13a)$$

and

$$\begin{aligned} [i\hbar\partial_t - e(\mathbf{k})] G_{\mathbf{k},m;i',m'}^{df}(t) &= V^* N_s^{-1/2} \\ &\quad \times \sum_j a_0^* \exp(-i\mathbf{k}\cdot\mathbf{R}_j) \\ &\quad \times G_{j,m;i',m'}^{ff}(t). \end{aligned} \quad (13b)$$

The equations of motion are then Fourier transformed, leading to the coupled set of algebraic equations

$$\begin{aligned} (\hbar\omega - \bar{E}_f) G_{\mathbf{k},m;\mathbf{k}',m'}^{ff}(\omega) &= \delta_{\mathbf{k},\mathbf{k}'} \delta_{m,m'} \\ &\quad + Va_0 G_{\mathbf{k},m;\mathbf{k}',m'}^{df}(\omega) \end{aligned} \quad (14a)$$

and

$$[\hbar\omega - e(\mathbf{k})] G_{\mathbf{k},m;\mathbf{k}',m'}^{df}(\omega) = V^* a_0^* G_{\mathbf{k},m;\mathbf{k}',m'}^{ff}(\omega). \quad (14b)$$

Since the Hamiltonian is quadratic these equations form a closed set and have the solution

$$G_{\mathbf{k},m;\mathbf{k}',m'}^{ff}(\omega) = \frac{\delta_{\mathbf{k},\mathbf{k}'}\delta_{m,m'}}{\{\hbar\omega - \tilde{E}_f - |Va_0|^2/[\hbar\omega - e(\mathbf{k})]\}} \\ = \delta_{\mathbf{k},\mathbf{k}'}\delta_{m,m'} \left[\frac{A_+(\mathbf{k})}{[\hbar\omega - E_+(\mathbf{k})]} + \frac{A_-(\mathbf{k})}{[\hbar\omega - E_-(\mathbf{k})]} \right] \quad (15a)$$

and

$$G_{\mathbf{k},m;\mathbf{k}',m'}^{df}(\omega) = \frac{Va_0\delta_{\mathbf{k},\mathbf{k}'}\delta_{m,m'}}{\{[\hbar\omega - e(\mathbf{k})](\hbar\omega - E_f) - |Va_0|^2\}} \\ = \frac{\delta_{\mathbf{k},\mathbf{k}'}\delta_{m,m'}A_+(\mathbf{k})A_-(\mathbf{k})}{\{[\hbar\omega - E_+(\mathbf{k})][\hbar\omega - E_-(\mathbf{k})]\}}, \quad (15b)$$

where we have expressed the Green's functions in terms of simple poles corresponding to two hybridized quasiparticle bands.

The two hybridized bands have dispersion relations given by

$$E_{\pm}(\mathbf{k}) = \{[\tilde{E}_f + e(\mathbf{k})] \pm \sqrt{[\tilde{E}_f - e(\mathbf{k})]^2 + 4\tilde{V}^2}\} / 2. \quad (16)$$

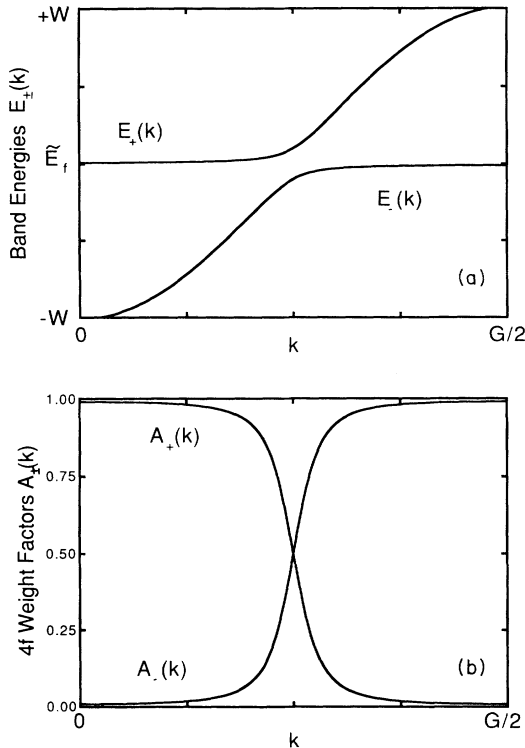


FIG. 1. The energy dispersion relations $E_{\pm}(\mathbf{k})$ for the hybridized bands found in the mean-field slave-boson approximation are shown as a function of \mathbf{k} in (a). The upper band and lower band indices are denoted by + and - respectively, and $\mathbf{G}/2 = \pi/a(1,1,1)$ is half a reciprocal lattice vector. The factors $A_{\pm}(\mathbf{k})$, which describe the $4f$ weight of the upper and lower hybridized bands, are plotted as functions of \mathbf{k} in (b).

These energy bands are sketched in Fig. 1(a). The factors $A_{\pm}(\mathbf{k})$ represent the $4f$ spectral weight contained in the Bloch state labeled by \mathbf{k} in the upper and lower hybridized bands, and these factors are given by

$$A_{\pm}(\mathbf{k}) = \frac{1}{2} \{ 1 \pm [\tilde{E}_f - e(\mathbf{k})] / \sqrt{[\tilde{E}_f - e(\mathbf{k})]^2 + 4\tilde{V}^2} \} \quad (17)$$

such that $A_+(\mathbf{k}) + A_-(\mathbf{k}) = 1$. These projection factors are depicted in Fig. 1(b). Here, \tilde{E}_f and \tilde{V} are given by renormalized expressions

$$\tilde{E}_f = E_f - \lambda_i \quad (18a)$$

corresponding to a shift in the binding energy of the f level, and

$$\tilde{V} = Va_0 \quad (18b)$$

is the reduced hybridization matrix element.

The renormalization of the f level energy may be understood as an energy lowering due to the zero-point motion from virtual hopping of the f electrons. Since a_0 is proportional to the square root of the number of $4f^0$ configurations, the factors of $4\tilde{V}^2$ occurring in the solution are reduced from their noninteracting values by the probability that the $4f$ level is already occupied. This reduction in the hopping probability is therefore due to the Coulomb interaction blocking the hopping of an electron onto a singly occupied f level, similar to the effect that occurs in the Gutzwiller effective band picture.^{27,28} Thus the slave-boson projection method prohibits a portion of the possible charge fluctuations from occurring, even as virtual states.

The two branches of quasiparticle poles form hybridized bands shown in Fig. 1(a). The two bands are separated by an indirect band gap between the lower band at $\mathbf{k} = \mathbf{G}/2$ and the upper band at $\mathbf{k} = 0$. The value of the gap is of the order of $4(Va_0)^2/W$, where W is the width of the d band. As shown in Fig. 1(b), for \mathbf{k} values close to the point $\mathbf{k} = 0$, the upper band is predominantly of $4f$ character and has an extremely flat slope, i.e., a high density of states. Likewise, for \mathbf{k} values near $\mathbf{k} = \mathbf{G}/2$, the lower band is also predominantly of f character and has a high density of states. Therefore, the indirect band gap occurs between states with predominantly $4f$ character. The minimum direct band gap is of order $(2Va_0)$. This occurs between states with equal f and d weights.

The f portion of these quasiparticle bands is subjected to a wave-function renormalization factor of $Z^{-1} = a_0^2$, which not only enhances the effective mass close to the localization transition^{27,28} but also has the effect of reducing the number of quasiparticles that can occupy the coherent quasiparticle bands to less than unity. If the Hamiltonian is rescaled in powers of N , the terms involving boson fluctuations may be ordered in powers of the boson propagator, which is of order $1/N$. In the large- N limit, these fluctuations may be neglected, resulting in this mean-field approach. The incoherent parts of the spectrum are higher order in $1/N$ since they involve the emission and absorption of slave bosons and are moved to energies further from the Fermi energy.

To obtain an insulating state, as in $\text{Ce}_3\text{Bi}_4\text{Pt}_3$ (Refs. 6

and 7), CeNiSn (Ref. 8), or YbB₁₂ (Refs. 9–11), one must be able to fill the lower hybridized band completely. Since the lower band contains half of the $2N$ states, one must have N electrons in total. It is interesting to note that for this occupation, the Anderson lattice model in the noninteracting limit ($U_{ff}=0$), would also be semiconducting. The results are consistent with the stability of the semiconducting state against the effect of interactions as implied by the argument's of Martin and Allen^{14,15} that involve Luttinger's theorem. However, since U_{ff} is considered to be infinite and a phase transition may occur, the prerequisite conditions needed for Luttinger's theorem to apply cannot be proved and possibly may not be satisfied.

We shall consider the case in which $N=2$ and extrapolate the mean-field theory, valid in the infinite- N limit, to the case where $N=2$. Then the number of electrons filling the lower band is half the total number of available states and is given by

$$N_{el} = 2N/2 = 2 .$$

The three self-consistency equations are as follows.

(i) The number of particles, which for the case in which the lower band is full, and the upper band is empty, is given by the equation

$$2N/2 = N = (1/N_s) \sum_{\mathbf{k}, \pm, m} f(E_{\pm}(\mathbf{k})) \quad (19)$$

since there is a total $2N$ states per atom, N d states and N f states, which are half filled. (In this expression, the non-quasiparticle f weight is counted.)

(ii) The constraint excluding multiply occupied configurations becomes

$$1 = a_0^2 + (1/N_s) \sum_{\mathbf{k}, \pm, m} A_{\pm}(\mathbf{k}) f(E_{\pm}(\mathbf{k})) . \quad (20)$$

(iii) The equation of motion for the stationary part of the slave-boson condensate yields

$$\lambda a_0 = -(V/N_s) \sum_{\mathbf{k}, m} A_{-}(\mathbf{k}) A_{+}(\mathbf{k}) \times [f(E_{-}(\mathbf{k})) - f(E_{+}(\mathbf{k}))] . \quad (21)$$

Since $VA_{-}(\mathbf{k})A_{+}(\mathbf{k})$ is of the order of $V^2 a_0 / |E_f - e(\mathbf{k})|$, λ can be seen to be an energy scale of the order of the zero-point energy for virtual hopping of the f electrons which is allowed when $a_0 \neq 0$.

The self-consistency equations have a nonzero solution for a_0 , in the range of temperatures below T_c . Above T_c the value of a_0 is zero. This can be seen directly from examination of two limiting cases.

A. High temperatures

The solution can be found, in the extreme high-temperature limit, since the Fermi functions become independent of the band index and quantum number \mathbf{k} ,

$$f(E_{\pm}(\mathbf{k})) = N_{el}/2N = \frac{1}{2} .$$

The constraint (20) becomes

$$a_0^2 = 1 - (N/N_s) \sum_{\mathbf{k}, \pm} A_{\pm}(\mathbf{k}) f(E_{\pm}(\mathbf{k})) = 1 - N_{el}/2 ,$$

and since there is a total of two electrons per ion, $N_{el}=2$, consisting of one f electron and one d electron per $4f$ ion, the gap equation (21) is trivially satisfied since it has a common multiplying factor of a_0 which is zero, $a_0=0$. The constraint then implies that in this high-temperature scale the number of f electrons is precisely unity.

B. Low temperatures

The solution in the zero-temperature limit $T=0$ is found with the use of the substitutions,

$$f(E_{-}(\mathbf{k})) = 1 \quad \text{and} \quad f(E_{+}(\mathbf{k})) = 0 ,$$

which occurs since the lower band is completely full and the upper band is empty. Thus, in the zero-temperature limit the constraint (20) becomes

$$1 = a_0^2 + (N/N_s) \sum_{\mathbf{k}} A_{-}(\mathbf{k}) , \quad (22)$$

which has a nontrivial solution when $E_f > 0$, that is $a_0^2 > 0$. The gap equation (21) reduces to

$$\tilde{E}_f - E_f = (V^2 N/N_s) \sum_{\mathbf{k}} \{ [\tilde{E}_f - e(\mathbf{k})]^2 + 4\tilde{V}^2 \}^{-1/2} .$$

For a structureless bare d band of width $2W$, the constraint can be written as

$$a_0^2 = (N/4W) [\sqrt{(W + \tilde{E}_f)^2 + 4\tilde{V}^2} - \sqrt{(W - \tilde{E}_f)^2 + 4\tilde{V}^2}] , \quad (23)$$

which has the solution

$$\tilde{E}_f = (\tilde{V}^2/N\Delta) [1 + 4N^2\Delta^2\tilde{V}^2 / (N^2\Delta^2W^2 - \tilde{V}^4)]^{1/2} , \quad (24)$$

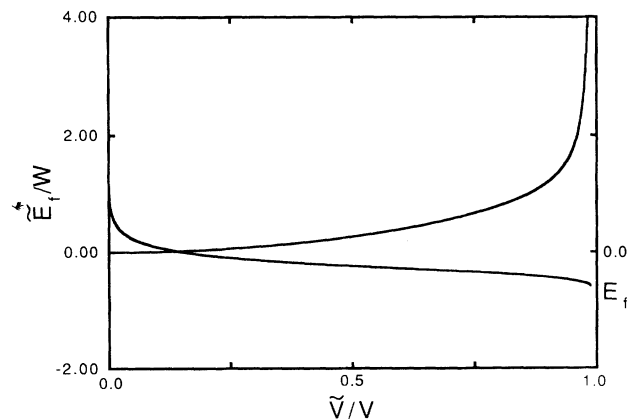


FIG. 2. The graphical solution of the self-consistency Eqs. (24) and (25). Both the expressions for \tilde{E}_f are plotted as a function of the hybridization matrix element renormalization factor \tilde{V}/V . The intersection of the two curves yields the renormalized values of \tilde{E}_f and \tilde{V} . Due to the singularities at $\tilde{V}=0$ and $\tilde{V}=V$, the equations always have a solution in which the effective hybridization matrix element is always smaller than the bare value.

where $\Delta = V^2/2W$ is a measure of the unrenormalized energy dispersion of the $4f$ states. For $N=2$, this equation has a singularity at $\tilde{V}=V$. The gap equation becomes

$$\begin{aligned} \tilde{E}_f - E_f = N\Delta \ln\{ [W + \tilde{E}_f + \sqrt{(W + \tilde{E}_f)^2 + 4\tilde{V}^2}] \\ \times [W - \tilde{E}_f \\ + \sqrt{(W - \tilde{E}_f)^2 + 4\tilde{V}^2}] / (4\tilde{V}^2) \}. \end{aligned} \quad (25)$$

After substituting (24) into Eq. (25), one finds that the resulting expression for \tilde{E}_f is singular at $\tilde{V}=0$. The pair of coupled equations (24) and (25) can be solved graphically and can be shown to always have a unique solution, with the position of the renormalized f level \tilde{E}_f above the center of the band. The graphical construction is shown in Fig. 2, where it can be seen that the presence of the two singularities ensures that the curves cross.

C. The critical temperature

The critical temperature T_c at which the boson condensation occurs is given by the condition $a_0^2=0$, which constrains the number of f electrons being unity, which in turn implies that the position of the renormalized f level \tilde{E}_f is exactly equal to zero. With these simplifications, the gap equation becomes

$$-E_f = (NV^2/N_s) \sum_{\mathbf{k}} [1 - 2f(e(\mathbf{k}))] / [2e(\mathbf{k})]. \quad (26)$$

The solution of the above equation yields the expression for the critical temperature,

$$k_B T_c = 1.14W \exp(E_f/N\Delta). \quad (27)$$

The exponent in the critical temperature given in (27) is the same as in the usual expression for the Kondo temperature T_K .

The order parameter a_0^2 is the deviation of the $4f$ occupation number from unity. The temperature variation is that of a mean-field transition, where the indirect hybridization gap in the electronic spectrum, proportional to a_0^2 opens up below T_c . The mean-field transition is controlled by the balance of the energy gained in opening up a gap at the Fermi level with the entropy from the spin disorder entropy of the high-temperature state. Due to the specific two-band nature of the electronic structure, the mean-field transition is gentle and is not accompanied by a discontinuity in the specific heat.

For values of the bare f level energy E_f far below the center of the band, the value of the low-temperature indirect gap E_{gap} is roughly $1.764k_B T_c$. In the other limit, when both the bare f level and the renormalized f level lie above the center of the band, the f level is mainly unoccupied, so the hybridization gap is not subjected to strong many-body reductions. At very low temperatures the gap shows an exponential temperature variation, with an exponent of $[E_-(\mathbf{G}/2) - \mu] / k_B T = [\mu - E_+(0)] / k_B T$, which since the Fermi energy lies in the center of the gap, has an activation energy of half the zero-temperature gap, or of the order of the critical tem-

perature. Thus, the activated behavior of the low-temperature thermodynamic properties does have a non-negligible contribution from the temperature variation of the gap in addition to the usual contribution from the thermal population of electrons or holes.

Although the system does show a phase transition in the mean-field approximation,¹⁹⁻²⁶ it is unclear if this will persist if the fluctuations in the slave-boson field are incorporated. As has been previously mentioned, the system may have a Goldstone mode that could restore the broken symmetry.^{20,21} However, one may argue that the stability of the low-temperature semiconducting phase^{13,14} is consistent with Luttinger's theorem and further speculate that if the fluctuations in the slave-boson field do destroy the phase transition, then only the gapped phase should remain. If the above speculation is indeed correct, the only remaining difference between the low- and high-temperature regimes would be in the magnitude of the gap.

IV. INELASTIC NEUTRON SCATTERING

The dynamic susceptibility is to be calculated within the mean-field slave-boson approximation. First, the spin operators are written as

$$S_{\mathbf{q}}^{\dagger} = N_s^{-1/2} \sum_{\mathbf{k}, m} C(m) f_{m+1, \mathbf{k}+\mathbf{q}}^{\dagger} f_{m, \mathbf{k}}, \quad (28a)$$

where $[C(m)]^2 = \hbar^2[(N^2 - 1)/4 - m(m+1)]$, and

$$S_{\mathbf{q}}^z = N_s^{-1/2} \sum_{\mathbf{k}, m} \hbar m f_{m, \mathbf{k}+\mathbf{q}}^{\dagger} f_{m, \mathbf{k}}. \quad (28b)$$

These expressions do not involve the slave-boson operators since the local spin operators do not involve a change in total f occupation at the site. The dynamic susceptibilities are then defined as

$$\chi_{\mathbf{q}}^{\alpha, \beta}(t) = (i/\hbar) \Theta(t) \langle [S_{\mathbf{q}}^{\alpha}(t), S_{-\mathbf{q}}^{\beta}(0)]_{-} \rangle, \quad (29)$$

which are then calculated from the equations of motion, in the slave-boson mean-field approximation. The imaginary part of the Fourier transform with respect to time is the spectral density of spin excitations and can be found, for sufficiently low frequencies, quite directly from inelastic-neutron-scattering cross sections.

The Fourier transforms of the dynamic susceptibility are found from the equation of motion. They are given by the expressions appropriate for noninteracting quasiparticles within the renormalized bands,

$$\begin{aligned} \chi_{\mathbf{q}}^{zz}(\omega) = \sum_{\mathbf{k}, m} \hbar^2 m^2 A_{\gamma}(\mathbf{k}+\mathbf{q})_m A_{\delta}(\mathbf{k})_m \\ \times [f(E_{\gamma}(\mathbf{k}+\mathbf{q})_m) - f(E_{\delta}(\mathbf{k})_m)] \\ \times [E_{\delta}(\mathbf{k})_m - E_{\gamma}(\mathbf{k}+\mathbf{q})_m - \hbar\omega]^{-1}, \end{aligned} \quad (30a)$$

$$\begin{aligned} \chi_{\mathbf{q}}^{+-}(\omega) = \sum_{\mathbf{k}, m} [C(m)]^2 A_{\gamma}(\mathbf{k}+\mathbf{q})_{m+1} A_{\delta}(\mathbf{k})_m \\ \times [f(E_{\gamma}(\mathbf{k}+\mathbf{q})_{m+1}) - f(E_{\delta}(\mathbf{k})_m)] \\ \times [E_{\delta}(\mathbf{k})_m - E_{\gamma}(\mathbf{k}+\mathbf{q})_{m+1} - \hbar\omega]^{-1} \end{aligned} \quad (30b)$$

and

$$\begin{aligned} \chi_q^{-+}(\omega) = & \sum_{\mathbf{k}, m} [C(m)]^2 A_\gamma(\mathbf{k}+\mathbf{q})_m A_\delta(k)_{m+1} \\ & \times [f(E_\gamma(\mathbf{k}+\mathbf{q})_m) - f(E_\delta(\mathbf{k})_{m+1})] \\ & \times [E_\delta(\mathbf{k})_{m+1} - E_\gamma(\mathbf{k}+\mathbf{q})_m - \hbar\omega]^{-1}. \end{aligned} \quad (30c)$$

In these expressions, the sums over γ and δ run over the upper and lower band indices independently. When the magnetic field B approaches zero, then these susceptibili-

$$\begin{aligned} J(\mathbf{q}) = & -4 \sum_{\mathbf{k}} |V(\mathbf{k}+\mathbf{q})|^2 |V(\mathbf{k})|^2 f_{\mathbf{k}}(1-f_{\mathbf{k}+\mathbf{q}}) / \{ [e(\mathbf{k}) - e(\mathbf{k}+\mathbf{q})][E_f - e(\mathbf{k}+\mathbf{q})]^2 \} \\ & - (1-f_{\mathbf{k}})(1-f_{\mathbf{k}+\mathbf{q}}) / \{ [E_f - e(\mathbf{k})]^2 [E_f - e(\mathbf{k}+\mathbf{q})] \}. \end{aligned} \quad (31)$$

This interaction has the same form as previously derived by other methods.³⁰ The first term is recognized³⁰ as the Ruderman-Kittel-Kasuya-Yosida (RKKY) interaction, in which the conduction spin density is polarized by the Schrieffer-Wolf interaction, and the second term is a form of Anderson superexchange interaction. Thus, by only retaining the subset of $1/N^2$ interactions and summing the effect of these exchange interactions to infinite order, one obtains a susceptibility in the usual random-phase approximation (RPA) form,

$$\chi_q^{+-}(\omega) = \hbar^2 \chi_q^0(\omega) / [1 - J(\mathbf{q})\chi_q^0(\omega)] \quad (32)$$

in which the noninteracting susceptibility $\chi_q^0(\omega)$ is given by an expression similar to those of Eq. (30). However, as the inclusion of these lowest-order exchange terms involves only a partial summation of a subset of terms in the entire $1/N$ series, the validity of this procedure is not well founded, and so we shall neglect these interaction effects entirely and only consider the susceptibility in the mean-field approximation.

The susceptibility will be examined above and below the mean-field transition temperature. At high temperatures, we shall see that the model yields the Curie susceptibility appropriate to independent magnetic moments, and at low temperatures we shall recover a susceptibility in the form of independent quasiparticles in renormalized (semiconducting) bands.^{27,28}

ties satisfy the relation $2\chi^{zz} = \chi^{\pm} = \chi^{\mp}$ expressing the spin rotational invariance of the paramagnetic state. Thus, magnetic ordering is not a consequence of the mean-field slave-boson approximation. The effect of magnetic exchange interactions between the f quasiparticles can be included, by considering diagrams of order $1/N^2$, and higher. These interactions have been considered by Doniach,²⁹ who has shown that if they are regarded as instantaneous, the exchange interactions are of separable form and are given by

A. High temperatures, $T > T_c$

The static susceptibility of the f electrons $\chi^{zz}(0)$ is reduced to a q -independent expression, since the renormalized dispersion of the $4f$ electrons vanishes. This is indicative of the local nature of the spins, and the static susceptibility becomes

$$\begin{aligned} \chi^{zz}(0) = & \hbar^2 [(N^2 - 1)/4] \\ & \times Nf(\tilde{E}_f)[1 - f(\tilde{E}_f)] / 3k_B T. \end{aligned} \quad (33)$$

Furthermore, since the average number of f electrons is one per $4f$ ion, $f(\tilde{E}_f) = 1/N$, then we recover the susceptibility of a set of independent local moments, to order $1/N$,

$$\chi^{zz}(0) = \hbar^2 (N^2 - 1)(1 - 1/N) / 12k_B T. \quad (34)$$

Thus, at high temperatures one recovers a Curie law due to the disordered spins on each $4f$ ion.

B. Low temperatures, $T < T_c$

At low temperatures, the f susceptibility acquires a significant q dependence. We shall display the limiting expressions for $\mathbf{q} = \mathbf{0}$, and $\mathbf{q} = (\pi/a)(1, 1, 1) = \mathbf{G}/2$.

The imaginary part of the dynamic susceptibility $\text{Im}\chi_q^{+-}(\omega)$ represents the spectral density of magnetic excitations involving a momentum change of \mathbf{q} . This is shown for $\mathbf{q} = \mathbf{0}$ in Fig. 3(a). For $\mathbf{q} = \mathbf{0}$, the imaginary part of the dynamic susceptibility may be written as

$$\begin{aligned} \text{Im}\chi_0^{+-}(\omega) = & \pi \hbar^2 (N^2 - 1) N \tilde{V}^2 / (6\omega \sqrt{\omega^2 - 4\tilde{V}^2}) \\ & \times (\rho(\tilde{E}_f + \sqrt{\omega^2 - 4\tilde{V}^2}) \{ f[\tilde{E}_f - \omega/2 + \sqrt{(\omega/2)^2 - \tilde{V}^2}] - f[\tilde{E}_f + \omega/2 + \sqrt{(\omega/2)^2 - \tilde{V}^2}] \} \\ & + \rho(\tilde{E}_f - \sqrt{\omega^2 - 4\tilde{V}^2}) \{ f[\tilde{E}_f - \omega/2 - \sqrt{(\omega/2)^2 - \tilde{V}^2}] - f[\tilde{E}_f + \omega/2 - \sqrt{(\omega/2)^2 - \tilde{V}^2}] \}) \end{aligned} \quad (35)$$

and the corresponding real part of the frequency-dependent susceptibility is given by

$$\text{Re}\chi_0^{+-}(\omega) = \rho(\tilde{E}_f) \hbar^2 (N^2 - 1) N \tilde{V}^2 \ln[(\omega - \sqrt{\omega^2 - 4\tilde{V}^2}) / (\omega + \sqrt{\omega^2 - 4\tilde{V}^2})] / (3\omega \sqrt{\omega^2 - 4\tilde{V}^2}) \quad (36a)$$

if $\omega > 2\tilde{V}$; whereas if $\omega < 2\tilde{V}$, then the alternate expression

$$\text{Re}\chi_0^{\pm}(\omega) = \rho(\tilde{E}_f) \hbar^2 (N^2 - 1) N \tilde{V}^2 \tan^{-1}[\omega / (4\tilde{V}^2 - \omega^2)^{1/2}] / (3/2\omega \sqrt{4\tilde{V}^2 - \omega^2}) \quad (36b)$$

holds at $T=0$. In these expressions, the excitation energy $\hbar\omega$ is denoted by ω . The $\mathbf{q}=0$ magnetic spectral density of Eq. (35) shows a threshold energy of order $2\tilde{V}$. This corresponds to the excitation of an electron from a state in the lower hybridized band to a state with the same momentum in the upper hybridized band, while flipping the spin of the electron. This direct gap $2\tilde{V}$ should also be observable in optical conductivity measurements of $\sigma(\omega)$ at low temperatures, if the indirect absorption processes are negligible. The spectral density is nonzero above the threshold and shows a characteristic square-root divergence at threshold; this square-root variation is similar to that found in the inelastic-neutron-scattering data of Aeppli⁸ on Ce-Ni-Sn systems.

The real part of the dynamic susceptibility, at finite frequencies also only has contributions from interband transitions. The real part of the $\mathbf{q}=0$ susceptibility is shown

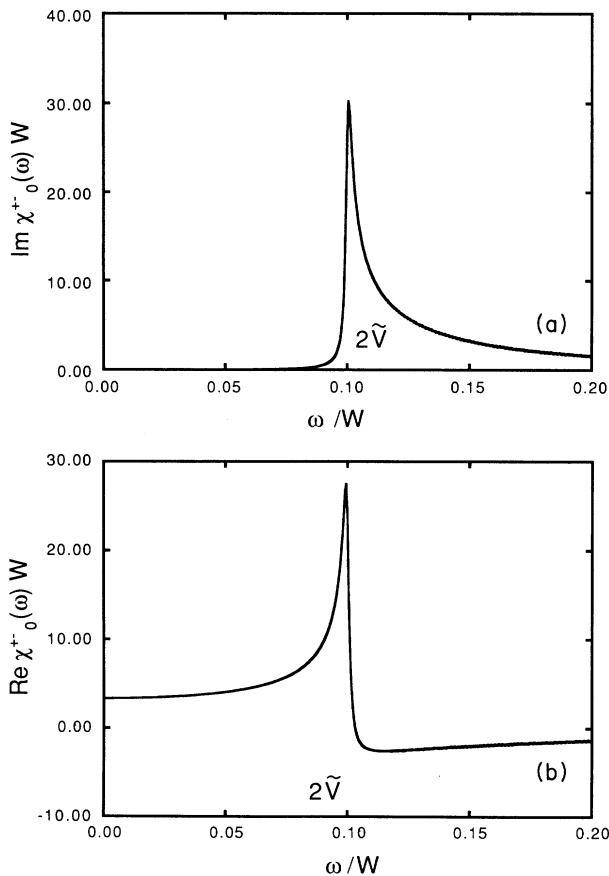


FIG. 3. The magnetic spectral density corresponding to the imaginary part of the dynamical susceptibility $\text{Im}\chi_{\mathbf{q}=0}^{\pm}(\omega)$ with $\mathbf{q}=0$, is shown (a) as a function of frequency ω . The spectrum only consists of an interband contribution that has a finite threshold energy $\hbar\omega=2\tilde{V}$. The corresponding real part of the dynamical susceptibility $\text{Re}\chi_{\mathbf{q}=0}^{\pm}(\omega)$ is shown in (b). Note that the $\omega=0$ limit does not yield the thermodynamic uniform static susceptibility, as the $\mathbf{q}=0$ and $\omega=0$ limits are not interchangeable.

in Fig. 3(b). At zero temperature it comes from electronic excitations from a completely filled, and therefore nonmagnetic, lower hybridized band to the upper hybridized band, which by virtue of the mixing matrix element has a $4f$ spin component. At zero frequency, $\omega=0$, and when the renormalized f level \tilde{E}_f is energetically degenerate with the nonhybridized b band, since the numerator is proportional to V^2 and the denominator is dominated by V^2 , the resulting value of the dc susceptibility is given approximately by the value of the nonhybridized d band density of states at the Fermi level $\rho(\tilde{E}_f)$. If the renormalized f level lies significantly above the upper d -band edge, one obtains a Van-Vleck-like contribution to the real part of the $\omega=0$ susceptibility of order $\tilde{V}^2/(\tilde{E}_f - W)$. We, therefore, shall designate the $T=0$ static susceptibility as a Van-Vleck-type term.

It should be noted that intraband excitations are prohibited from occurring in the $\mathbf{q}=0$ dynamic susceptibility for finite ω values. They do occur at finite temperatures in the uniform static susceptibility, where the order of the \mathbf{q} and ω limits are interchanged, and this coincides with the usual definition of the static susceptibility as the second derivative of the free energy with respect to field. The interband Van Vleck contribution to the static susceptibility is recognized to occur as a result of the magnetic field changing the f spectral weight admixture factors $A_{\pm}(\mathbf{k})_m$ in the expression for the magnetization due to the f moments. This is supportive of the nomenclature that we have adopted. The intraband contribution requires the existence of a thermal population of electrons in the upper hybridized band, or holes in the lower hybridized band. Therefore, they do not contribute to

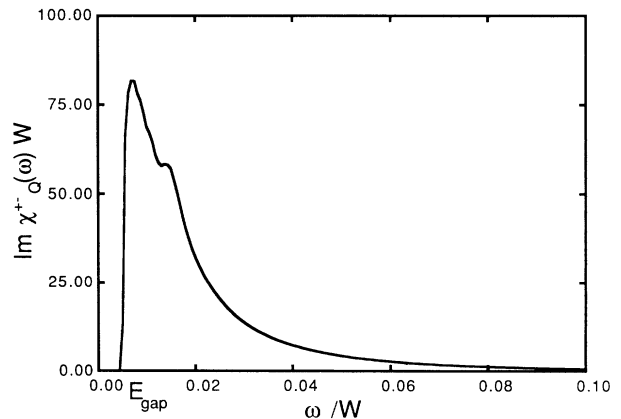


FIG. 4. The magnetic spectral density calculated for $\mathbf{q}=\mathbf{G}/2=(\pi/a)(1,1,1)$, as a function of frequency ω . The spectrum exhibits a threshold for the interband contributions at $\hbar\omega \approx 2\tilde{V}^2/W$, and a low-intensity quasielastic (interband) contribution can be seen below the threshold. The anomaly in the spectrum seen above the threshold energy is just due to the Van Hove anomaly in the three-dimensional tight-binding density of states used to describe the unhybridized d band.

the static susceptibility at zero temperature and are thermally activated for temperatures less than the transition temperature or half the indirect band gap. The susceptibility peaks at temperatures of the order of the indirect band gap, where the presence of electron hole pairs has metallized the f component of the density of states.

The gap in the spin-flip scattering spectrum is minimized at $\mathbf{q}=\mathbf{G}/2=(\pi/a)(1,1,1)$. This value of the gap E_{gap} should be the same as the thermodynamic gap as observed in resistivity, specific heat experiments, which can

be approximated by the value

$$E_{\text{gap}}=2W\tilde{V}^2/(W^2-\tilde{E}_f^2) \quad (37)$$

when $W \gg \tilde{E}_f$. This indirect gap E_{gap} is much smaller than the direct gap of $2\tilde{V}$ found in the spectral density calculated with $\mathbf{q}=\mathbf{0}$.

An analytic expression for the dynamical susceptibility at $\mathbf{q}=\mathbf{G}/2$ can be found using a tight-binding approximation for the d -band dispersion relation, and this is given by

$$\begin{aligned} \text{Im}\chi_{\mathbf{q}}^{+-}(\omega) &= \hbar^2(N^2-1)(N/6) \{ \pi\rho(e(\mathbf{k}))A_-(\mathbf{k}+\mathbf{q})A_+(\mathbf{k})[f(E_-(\mathbf{k}+\mathbf{q}))-f(E_+(\mathbf{k}))]/[A_+(\mathbf{k}+\mathbf{q})+A_-(\mathbf{k})]|_{\epsilon} \\ &\quad + \pi\rho(e(\mathbf{k}))A_-(\mathbf{k}+\mathbf{q})A_-(\mathbf{k})[f(E_-(\mathbf{k}+\mathbf{q}))-f(E_-(\mathbf{k}))]/[A_+(\mathbf{k}+\mathbf{q})+A_+(\mathbf{k})]|_{\epsilon} \\ &\quad + \pi\rho(e(\mathbf{k}))A_+(\mathbf{k}+\mathbf{q})A_+(\mathbf{k})[f(E_+(\mathbf{k}+\mathbf{q}))-f(E_+(\mathbf{k}))]/[A_-(\mathbf{k}+\mathbf{q})+A_-(\mathbf{k})]|_{\epsilon} \} , \end{aligned} \quad (38a)$$

where the energies satisfy the perfect nesting relations $e(\mathbf{k})=-e(\mathbf{k}+\mathbf{q})$ and are given by the three solutions of the cubic equation for e ,

$$\begin{aligned} 2\omega e^3 + (4\tilde{V}^2 - 5\omega^2)e^2 - 2\omega(\tilde{E}_f^2 + 4\tilde{V}^2 - 2\omega^2)e \\ + \omega^2(\tilde{E}_f^2 + 4\tilde{V}^2 - \omega^2) = 0 . \end{aligned} \quad (38b)$$

The first term of (38a) represents the interband contribution, and the second and third terms represent the intraband contributions. A typical form of the magnetic spectral density for $\mathbf{q}=\mathbf{G}/2$ is shown in Fig. 4.

At zero temperatures, when the lower hybridized band is completely filled and the upper hybridized band is empty, the only excitations that can occur are spin-flip excitations involving the removal of an electron from the lower hybridized band and replacing it in the upper hybridized band with a momentum increased by $\mathbf{G}/2$. The threshold excitation energy for these processes is E_{gap} , below which the spin spectral density is zero. The anomaly in the magnetic spectrum seen in Fig. 4 just above the threshold energy is just a manifestation of the Van Hove anomaly in the three-dimensional tight-binding density of states used for the d electrons. A useful approximation for the interband contribution to the susceptibility, valid

in the strongly renormalized regime where $\tilde{E}_f \approx 0$, is given by

$$\begin{aligned} \hbar^2(N^2-1)N(4\tilde{V}^2)^2\pi\rho((\omega^2-4\tilde{V}^2)/2\omega) \\ \times [f(-\omega)-f(\omega)]/12\omega^2(\omega^2+4\tilde{V}^2) . \end{aligned} \quad (39)$$

At finite temperatures and $\mathbf{q}=\mathbf{G}/2$, the spin spectral density shows a quasielastic peak within the band gap. This corresponds to intraband scattering of thermal population of holes in the lower hybridized band, or of intraband scattering of the thermal population of electrons in the upper hybridized band. Since there is no threshold for intraband scattering processes, the quasielastic peak extends down to zero. The quasielastic peak in the dynamic susceptibility vanishes at $\omega=0$ in order to satisfy the fluctuation dissipation theorem. Since the quasielastic scattering involves the thermal population of electrons in the upper hybridized band or holes in the lower hybridized band, the total integrated intensity should be proportional to the number of thermally excited electron hole pairs or just the number of holes. A useful approximation for the intraband terms, valid in the strongly renormalized regime where $\tilde{E}_f \approx 0$, is given by

$$\begin{aligned} \pi\hbar^2(N^2-1)N\rho(\omega) \{ \tilde{V}^2/[6(\omega^2+4\tilde{V}^2)] \} [f(-\frac{1}{2}(\omega-\sqrt{\omega^2+4\tilde{V}^2}))+f(-\frac{1}{2}(\omega+\sqrt{\omega^2+4\tilde{V}^2})) \\ -f(\frac{1}{2}(\omega+\sqrt{\omega^2+4\tilde{V}^2}))-f(\frac{1}{2}(\omega-\sqrt{\omega^2+4\tilde{V}^2}))] . \end{aligned} \quad (40)$$

When considered as a function of temperature the intraband contribution always remains relatively small, since it is thermally activated at low temperatures and is also dominated by \tilde{V}^2 , which is small and indeed vanishes at T_c . Furthermore, when regarded as a function of frequency, one sees that for frequencies in the range that maximize the Fermi function factors $\hbar\omega \approx W$, the d -band density of states $\rho(\omega)$ becomes vanishingly small. Hence the intensity of the intraband contribution remains low, although it is distributed over a wide range of energies $\hbar\omega$.

C. Experiments

The measured static susceptibility^{6,7} of $\text{Ce}_3\text{Bi}_4\text{Pt}_3$ is shown in Fig. 5. The susceptibility shows a Curie tail at low temperatures, probably caused by local impurities with magnetic moments. This suggestion seems to be confirmed from the Kramers-Kronig analysis of the inelastic-neutron-scattering experiments, which indicates that the $\mathbf{q}=\mathbf{0}$ susceptibility should saturate to a low-temperature value of roughly 2×10^{-3} emu per mole Ce. Thus one expects that the $T=0$ value of the susceptibility

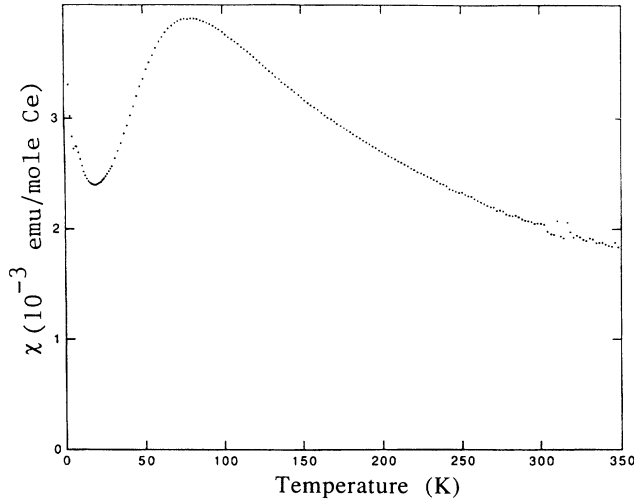


FIG. 5. The measured static susceptibility for $\text{Ce}_3\text{Bi}_4\text{Pt}_3$ as a function of temperature. The data is taken from Ref. 6. The low-temperature upturn is probably caused by magnetic impurities.

should be close to the value of the low-temperature minimum found in the thermodynamic measurements. This inferred $T=0$ value therefore should directly correspond to the theoretically calculated Van Vleck interband contribution susceptibility. Since the value of this susceptibility is moderately large, this implies that the nonhybridized density of states at the renormalized f level energy \tilde{E}_f is high. The intraband contribution, due to the thermal population of holes at finite T , vanishes at $T=0$ and gives rise to peak at finite T . The peak occurs at temperatures a quarter of the critical temperature, as can be seen in Fig. 6. With this finite concentration of electron hole pairs, the intraband contribution to the sus-

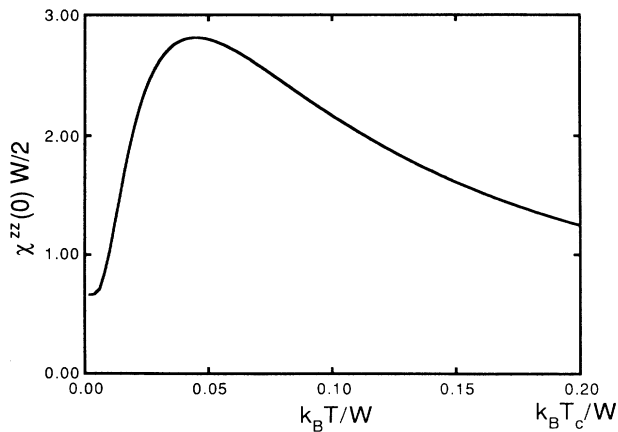


FIG. 6. The calculated temperature dependence of the static susceptibility, in units of half the band width, as a function of $k_B T/W$. At zero temperatures, the susceptibility is of a Van Vleck origin, whereas at higher temperatures the susceptibility is that associated with a metal composed of a gas of thermally excited heavy electrons or holes.

ceptibility is metallic and is comparable to the susceptibility of a moderately enhanced heavy-fermion metal.

The spin-flip contribution to the inelastic-neutron-scattering cross section is proportional to the factor

$$[1 - \exp(-\hbar\omega/k_B T)]^{-1} \text{Im}\chi_q^{+-}(\omega). \quad (41)$$

This scattering cross section was measured for $\text{Ce}_3\text{Bi}_4\text{Pt}_3$ by Severing *et al.*⁶ on powdered samples. As only the average neutron momentum transfer \mathbf{q} can be determined, we have compared these results with the analytic expression derived with $\mathbf{q}=\mathbf{G}/2$. In doing this we are presuming that the average spin spectral density is heavily weighted for these \mathbf{q} values. The inelastic-scattering cross section measured at $T=2$ K is shown in Fig. 7. The data clearly shows an energy gap of the order of 12 meV and no thermally induced quasielastic states within the gap, consistent with the $T=0$ mean-field theory. The inelastic-scattering data taken at $T=50$ K is not quite so clear cut, as seen in Fig. 8. The spectrum extends down to zero energies suggesting the existence of a quasielastic contribution. The high-energy portion of the spectrum appear to have shifted to lower energies indicating a temperature-dependent reduction of the gap.

The effects of magnetic exchange interactions^{29,30} included through Eqs. (31) and (32) could lead to some interesting effects. First, the square-root singularity in the $\mathbf{q}=0$ inelastic-neutron-scattering spectrum is expected to have the leading edge of the singularity replaced by a square-root approach to zero at the threshold of $\hbar\omega=2\tilde{V}$. Second, there exists the possibility of a dispersive collective mode occurring in the spectrum, either as a resonance within the continuum of electron hole spin-flip excitations or as a branch of bound states split off below the edge of the continuum. At low temperatures, the branch of bound states should show up as a narrow inelastic peak within the gap. Due to the large strength of the magnetic exchange interaction for $\mathbf{q}=\mathbf{G}/2$, for values of the chemical potential close to the center of the band, this structure might be most clearly resolved from the band edge in the low-energy inelastic-neutron-scattering experiments with momentum transfers of $\mathbf{q}=\mathbf{G}/2$. However, no such structure could be resolved in the gap found in the exper-

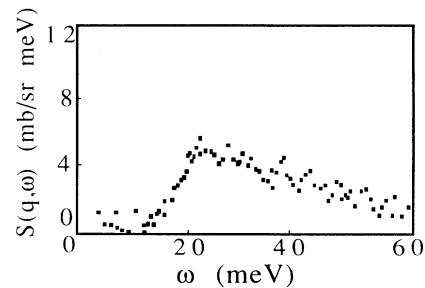


FIG. 7. The inelastic-neutron-scattering cross section for $\text{Ce}_3\text{Bi}_4\text{Pt}_3$, from Ref. 6, as a function of neutron energy transfer $\hbar\omega$ at $T=2$ K. The spectrum clearly shows a gap in the spectrum at energies $\hbar\omega \approx 15$ meV. The spectrum has a shape similar to that found in the calculation at $\mathbf{q}=\mathbf{G}/2$.

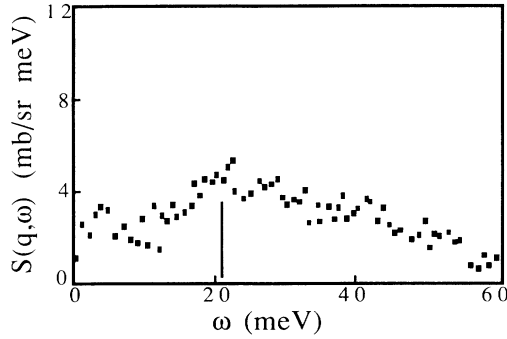


FIG. 8. The inelastic-neutron-scattering cross section measured at $T=50$ K, from Ref. 6. The threshold energy found at $T=2$ K is marked by an arrow. No evidence of the gap remains, and the high-energy tail of the spectrum has moved to lower energies. This is argued to be indicative of the closing of the gap, instead of the filling of the gap with a thermally activated quasielastic (intraband) peak.

imentally determined spectrum.

Other evidence concerning the existence of a gap comes from the low-temperature specific heat which is much smaller than the corresponding specific heat of the Lanthanum homolog. This indicates that the electronic density of states at the Fermi level is 3.3 mJ/mole Ce K^2 , which is a factor of 3 less than that of $La_3Bi_4Pt_3$, which contains no f electron density of states at the Fermi energy. The form of the specific heat, calculated within the mean-field approximation, is shown in Fig. 9. The resistivity shows thermal activated behavior. Assuming an Arrhenius law, the logarithmic plot versus $1/T$ shows a gap that increases with decreasing temperature, consistent with the mean-field theory.^{6,7} The low-temperature value of the activation energy found in thermodynamic properties is a factor of 2 less than the gap E_{gap} found in the inelastic-neutron-scattering experi-

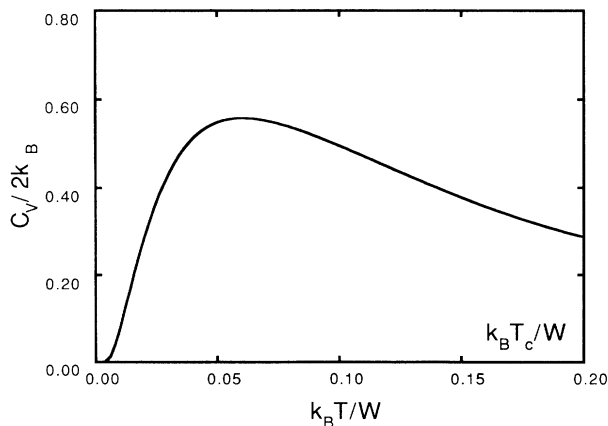


FIG. 9. The calculated temperature dependence of the specific heat, as a function of $k_B T/W$. The specific heat vanishes at $T=0$, due to the existence of a gap in the excitation spectrum. At higher temperatures, the specific heat takes on the form associated with a heavy-fermion system.

ments. However, in a semiconductor at low temperatures, thermodynamic quantities typically shows thermally activated variations that depend upon the excitation energy measured from the chemical potential; the latter lies in the center of the gap. Thus, the number of thermally excited electrons should have an activation energy of

$$E_+(G/2) - \mu = E_{gap}/2 \approx \tilde{V}^2/W,$$

which is consistent with the observations.

These systems should show very interesting effects connected with the modifications induced by impurity doping, which may lead to the destruction of coherence and the appearance of local states within the hybridization gap.³¹ The increase in the concentration of non-bound-state electrons will also produce a shift of the Fermi level relative to the edge of the hybridization gap. This disorder-induced metallic phase should show properties reminiscent of the $T=0$ heavy-fermion metals. This type of behavior would be direct confirmation that these materials support a novel kind of heavy-fermion state, the heavy-fermion semiconductor. In fact these experiments have already been performed,¹² Lanthanum doping of $Ce_3Bi_4Pt_3$ leads to linear T specific heat coefficients of the order of 150 mJ/mole Ce K^2 , which is of the order of magnitude associated with moderately enhanced heavy-fermion systems. If the effect of localization can be neglected, the above mean-field theory predicts that there should be a strong asymmetry between the effects of electron and hole doping that should be apparent in the limit of large impurity concentrations. The origin of this asymmetry is simply due to the fact that the Coulomb interaction forbids doping by more than one electron per f ion, whereas no such restriction occurs for hole doping. In the case of doping with one electron per $4f$ ion, then the system is chemically inert and the $4f$ ions remain integrally occupied, localized and incoherent at all temperatures. For doping with one $4f$ electron per ion the $4f$ occupancy may range between the limits of unity and zero, and the behavior of the system may accordingly range from fully hybridized and coherent, to localized and incoherent. For arbitrary values of doping and asymmetry should show up in the magnitude of the low-temperature wave function or mass renormalization, the mass renormalization should be larger for electron doping than for the corresponding case of hole doping.

V. CONCLUSIONS

The slave-boson mean-field theory shows a transition, below a critical temperature T_c , from a local-moment regime to a state with hybridized bands separated by an indirect band gap. If this system contains enough electrons to fill the lower hybridized band, then the system will undergo a transition from a high-temperature metal, with spin disorder scattering, to a low-temperature semiconductor. This transition is due to slave-boson condensation and may be expected to be smoothed out due to phase fluctuations. However, the Luttinger theorem arguments made by Martin and Allen^{14,15} seem to suggest that the low-temperature semiconducting phase should

be stable against the effect of interactions. Thus, one may speculate that the effect of higher-order fluctuations will merely diminish the gap at higher temperatures and not cause it to completely vanish.

The inelastic-neutron-scattering cross section should show a gap at low temperatures, and the allowed transitions correspond to exciting an electron from the lower hybridized band to the upper, and flipping its spin. At finite temperatures, the magnitude of the gap should decrease and a quasielastic scattering cross section should occur. This latter is due to the finite thermal population of electrons in the upper hybridized band or holes in the lower band. The inelastic-neutron-scattering spectrum of $\text{Ce}_3\text{Bi}_4\text{Pt}_3$ has been compared with predictions of the

theory. The results are suggestive of the existence of a band gap at $T=2$ K and that the gap closes at higher temperatures, although no clear separation of the quasi-elastic from the inelastic scattering has been made.

ACKNOWLEDGMENTS

The author would like to acknowledge enlightening and stimulating conversations with Dr. A. M. Boring, Dr. P. C. Canfield, Dr. Z. Fisk, Dr. S. Horn, Dr. J. M. Lawrence, Dr. G. R. Stewart, and last but not least Dr. J. D. Thompson. This work was supported by a grant from the U.S. Department of Energy, Office of Basic Energy Sciences.

-
- ¹G. R. Stewart, *Rev. Mod. Phys.* **56**, 755 (1984).
²P. A. Lee, T. M. Rice, J. W. Serene, L. J. Sham, and J. W. Wilkins, *Comments Condens. Matter Phys.* **3**, 99 (1986).
³D. M. Newns and N. Read, *Adv. Phys.* **36**, 799 (1987).
⁴P. Fulde, J. Keller, and G. Zwirgner, *Solid State Phys.* **41**, 1 (1988).
⁵A. Jayaraman, V. Narayanamurti, E. Bucher, and R. G. Maines, *Phys. Rev. Lett.* **25**, 1430 (1970).
⁶A. Severing, J. D. Thompson, P. C. Canfield, Z. Fisk, and P. S. Riseborough, *Phys. Rev. B* **44**, 6832 (1991).
⁷M. F. Hundley, P. C. Canfield, J. D. Thompson, Z. Fisk, and J. M. Lawrence, *Phys. Rev. B* **42**, 6842 (1990).
⁸G. Aeppli, private communication.
⁹T. Takabatake, F. Teshina, H. Fujii, S. Nishigori, T. Suzuki, T. Fujita, Y. Yamaguchi, J. Sakurai, and D. Jaccard, *Phys. Rev. B* **41**, 9607 (1990).
¹⁰T. Kasuya, F. Iga, M. Takigawa, and T. Kasuya, *J. Magn. Magn. Mat.* **47&48**, 429 (1985).
¹¹K. Sugiyama and M. Date, *Physica B* **155**, 253 (1989).
¹²J. D. Thompson, private communication.
¹³C. M. Varma and Y. Yaffet, *Phys. Rev. B* **13**, 2950 (1976).
¹⁴R. M. Martin and J. W. Allen, *J. Appl. Phys.* **50**, 7561 (1979); **53**, 2143 (1980).
¹⁵R. M. Martin and J. W. Allen, *Phys. Rev. Lett.* **48**, 362 (1982).
¹⁶N. Grewe and H. Keiter, *Phys. Rev. B* **24**, 4420 (1981).
¹⁷S. E. Barnes, *J. Phys. F* **6**, 1375 (1976).
¹⁸P. Coleman, *Phys. Rev. B* **29**, 3035 (1984).
¹⁹N. Read and D. M. Newns, *Solid State Commun.* **52**, 993 (1984).
²⁰P. Coleman, *J. Magn. Magn. Mater.* **47&48**, 323 (1985).
²¹P. Coleman, *Phys. Rev. B* **35**, 5072 (1987).
²²Z. Tesanovich and O. Valls, *Phys. Rev. B* **34**, 1918 (1986).
²³A. J. Millis and P. A. Lee, *Phys. Rev. B* **35**, 3394 (1987).
²⁴J. W. Rasul and H. U. DesGranges, *J. Phys. C* **19**, L671 (1986).
²⁵S. M. Evans, T. Chung, and G. A. Gehring, *J. Phys. C* **1**, 10473 (1989).
²⁶N. Grewe and T. Pruschke, *Z. Phys. B* **60**, 311 (1985).
²⁷W. F. Brinkman and T. M. Rice, *Phys. Rev. B* **2**, 4302 (1970).
²⁸T. M. Rice and K. Ueda, *Phys. Rev. Lett.* **55**, 995 (1985); see also, C. M. Varma, W. Weber, and L. J. Randall, *Phys. Rev. B* **33**, 1015 (1986).
²⁹S. Doniach, *Phys. Rev. B* **35**, 1814 (1987).
³⁰P. S. Riseborough, *Solid State Commun.* **55**, 755 (1985).
³¹R. Sollie and P. Schlottmann, *J. Appl. Phys.* **69**, 5478 (1991).